Original article

Nuclear Medicine Communications

Biodistribution and internal dosimetry of the ^{188}Re-labelled humanized monoclonal antibody anti-epidemal growth factor receptor, nimotuzumab, in the locoregional treatment of malignant gliomas

Leonel A. Torres[a], Marco A. Coca[a], Juan F. Batista[a], Angel Casaco[b], Gerardo Lopez[c], Ivan García[c], Alejandro Perera[a], Yamilé Peña[a], Abel Hernández[a], Yolaine Sanchez[a], Susana Romero[a], Rene Leyva[d], Anais Prats[a] and Ramses Fernandez[c]

Objective **To evaluate the biodistribution, internal radiation dosimetry and safety of the ^{188}Re-labelled humanized monoclonal antibody nimotuzumab in the locoregional treatment of malignant gliomas.**

Methods **Single doses of 370 or 555 MBq of ^{188}Re-labelled nimotuzumab were locoregionally administered to nine patients with recurrent high-grade gliomas, according to an approved dose-escalation study. SPECT, planar scintigraphy and magnetic resonance images were combined for dosimetric and pharmacokinetic studies. Blood and urine samples were collected to evaluate clinical laboratory parameters and for absorbed doses calculations. Biodistribution, internal dosimetry, human anti-mouse antibody response and toxicity were evaluated and reported.**

Results **The ^{188}Re-nimotuzumab showed a high retention in the surgically created resection cavity with a mean value of 85.5 ± 10.3%ID 1 h post-injection. It produced mean absorbed doses in the tumour region of approximately 24.1 ± 2.9 Gy in group I (patients receiving 370 MBq) and 31.1 ± 6.4 Gy in group II (patients receiving 555 MBq); the normal organs receiving the highest absorbed doses were the kidneys, liver and urinary bladder. About 6.2 ± 0.8%ID was excreted by the urinary pathway. The maximum tolerated dose was 370 MBq because two patients showed severe adverse effects after they received 555 MBq of ^{188}Re-nimotuzumab. No patient developed human anti-mouse antibody response.**

Conclusions **A locoregional single dose of ^{188}Re-labelled nimotuzumab of approximately 370 MBq could be used safely in the routine treatment of patients suffering with high-grade gliomas. The efficacy of this therapy needs to be evaluated in a phase II clinical trial.** ***Nucl Med Commun*** **29:66–75 © 2008 Wolters Kluwer Health | Lippincott Williams & Wilkins.**

Nuclear Medicine Communications 2008, **29**:66–75

Keywords: radioimmunotherapy, dosimetry, biodistribution, nimotuzumab, h-R3

Centres for [a]Clinical Researches, [b]Molecular Immunology, [c]International Centre of Neurological Restoration and [d]Centre of Isotopes, Havana, Cuba

Correspondence to Leonel A. Torres, Centre for Clinical Researches, Calle 34 No. 4501 e/ 45 y 47, Rpto Kohly, PO Box 11300, Playa, C. Havana, Cuba
Tel: +53 7202 3763; fax: +53 7204 3298;
e-mail: leonel@infomed.sld.cu

Received 7 May 2007 **Revised** 30 May 2007
Accepted 3 September 2007

Introduction

Locoregional radioimmunotherapy (LR-RIT) of brain tumours using molecules labelled with β-emitters has been proposed as part of a combined modality approach in order to improve the prognosis for these patients [1,2]. Positive clinical responses were achieved by many groups using direct injection of ^{131}I- or ^{90}Y-labelled peptides, fragments or monoclonal antibodies (MAbs) into the surgically created resection cavity (SCRC) [3–5]. Most of the reported studies using this treatment modality have been carried out using BC-2, BC-4 and 81C6 molecules which bind with high affinity to tenascin, an extracellular matrix glycoprotein overexpressed in malignant gliomas [1–3].

Labelled anti-epidermal growth factor receptor (EGFr) MAbs have also been used for treatment of brain tumours since Epenetos *et al.*, in 1985, administered intra-arterially the ^{131}I-labelled 9A MAb to a patient who suffered from a recurrent grade IV glioma [6]. Later, various clinical trials were performed to evaluate the use of ^{125}I-labelled murine anti-EGFr MAb 425, administered intravenously to patients suffering from brain tumours; this treatment demonstrated an increment in the survival times of about 180 patients [7].

The humanized monoclonal antibody nimotuzumab is a genetically engineered IgG1 obtained from the murine

MAb ior egf/r3, with high affinity ($K_d = 10^{-8}$ mol·l^{-1}) and specificity to the EGFr [8]. Several pre-clinical and clinical trials have shown the safety and efficacy of this molecule and its parent MAb for diagnostic and therapeutic purposes [9–13]. These results have suggested the potential usefulness of nimotuzumab labelled with β-emitters for LR-RIT of high-grade gliomas.

The radionuclide ^{188}Re (half-life of 17 h) is easily obtained from a ^{188}W generator and is considered to be an excellent β-emitting radionuclide that also allows for imaging with scintigraphy. Its γ-emissions (155 keV), with 15% abundance, and the high-energy of the β emissions (E_{max} of 2.12 MeV) combine the deliverance of high doses to malignant tissues and imaging for biodistribution and dosimetric purposes, enhancing the evaluation of the radiological patient safety [14]. Taking into account the advantages of ^{188}Re for radionuclide therapy and the results of previous clinical studies using this radionuclide [15], the radioimmunoconjugated ^{188}Re-nimotuzumab was proposed for LR-RIT of brain tumours. The labelling procedures were previously established and optimized [16].

The main goal of this study was to evaluate the biodistribution, internal radiation dosimetry and toxicity of the ^{188}Re-labelled humanized MAb nimotuzumab, administered locoregionally to patients bearing high-grade gliomas.

Materials and methods

Study design and patient inclusion

A phase I, open-label, uncontrolled, prospective and dose-escalation study was evaluated and approved by the national regulatory authorities and the institutional review boards involved. The primary end-point of this study was to evaluate the safety, biodistribution and internal dosimetry of the radioimmunoconjugated ^{188}Re-nimotuzumab used for LR-RIT of gliomas grade III or IV.

Patients previously treated with conventional procedures (surgery and external radiotheraphy) who presented recurrent disease were eligible for this study. The inclusion criteria were as follows: histologically demonstrated EGFr overexpression on a recurrent high-grade glioma, Karnofsky performance status > 70, life expectancy of at least 6 months, age between 18 and 75 years, normal hepatic and renal function, and haematological parameters in a normal range. Written informed consent was required from all patients.

Dose escalations were performed according to a modified Fibonacci schema. Three milligrams of nimotuzumab MAb were labelled with different amounts of ^{188}Re, starting from 370 MBq with increments of 185 MBq. Each dose level would include three patients if no adverse effects would have appeared. If two patients presented severe adverse effects then the next level would not be evaluated. However, three additional patients would be included in the previous dose level to provide more evidence about its safety.

Monoclonal antibody

The humanized MAb nimotuzumab was supplied by the Centre of Molecular Immunology, Havana, Cuba, in vials with 5 mg·ml^{-1}. This MAb is a human IgG1 directed against human EGFr. It was reconstructed from the murine MAb ior egf/r3 as described previously by Mateo *et al.* [8].

Monoclonal antibody labelling and quality control

MAb nimotuzumab was directly labelled by the Schwarz and Steinstraber method [17]. A 2000-fold molar excess of 2-mercaptoethanol was added to 5 mg of nimotuzumab and incubated for 30 min at room temperature. The antibody was purified through a gel filtration PD-10 column (Pharmacia–Amersham, UK), eluted with nitrogen purged 0.01 mol·l^{-1} PBS pH = 8.2. Two millilitres of a solution containing 1.82 mmol·l^{-1} of sodium glucoheptonate, 0.26 mmol·l^{-1} of ascorbic acid and 32 mmol·l^{-1} of stannous fluoride were added to 3 mg of reduced nimotuzumab. Then, 555–740 MBq of ^{188}Re was added and the mixture was incubated for 3 h at room temperature.

The amounts of free perrhenate and labelled glucoheptonate (as percent) were assessed by paper chromatography as reported by Perera *et al.* [16].

Administration of antibody

A Rickman or Ommaya intra-cavitary catheter with a subcutaneous reservoir was installed in all patients during the craniotomy procedure. After verifying the catheter viability, the ^{188}Re-nimotuzumab radioimmunoconjugate was administered as a bolus injection in a volume of 2–4 ml, and 1 ml of saline solution was added in order to decrease the remaining activity in the reservoir reducing irradiation of the scalp. All patients received prophylactic treatment including dexamethasone 8–16 mg per day, 72 h before the administration, and diuretic drugs to increase the clearance of the activity.

Determination of toxicity

All patients were monitored after the radioimmunoconjugate injection for any adverse event. Vital signs were also evaluated and registered at different time intervals. Special attention was given to the detection of neurological symptoms and signs that could be related to neurological radiotoxicity. The Common Toxicity Criteria of the National Cancer Institute were used to classify the adverse events being scaled as mild, moderate, severe or very severe.

Complete blood cell counts with differential and platelet examination, chemistry panel evaluation, liver function tests and urine analyses were performed weekly for the first 8 weeks post-injection. Data were analysed in order to identify signs of haematological or normal tissue toxicity. Human anti-mouse antibody responses (HAMA) were measured during the first 6 months post-injection as previously reported [11].

Biodistribution studies

Four sets of planar images (including emission, scatter and attenuation studies) were collected from all patients using a γ camera (Sophy DS7 Camera; Sophy, France) controlled by a Mirage workstation (Segami Corporation, USA). The detector was fitted with a parallel-hole collimator (360 keV) and emission images were acquired using a 20% window centred at 155 keV of the ^{188}Re spectrum. Two adjacent scatter windows (10% windows) were located at 133 and 180 keV in order to perform scatter correction using the triple-windows energy method, as previously reported [14]. Transmission images were acquired from the head and abdomen to compute the attenuation correction coefficients of the main source organs and regions, using a ^{99m}Tc-filled flood phantom. Anterior and posterior static views of the whole body (head, thoracic, abdominal and pelvic views) were acquired at 1, 5, 24 and 48 h after administration of the radiopharmaceutical.

The studies were processed according to well-established procedures [18,19]. The total uptake of normal organs and tumours at different time intervals were computed and reported as percent of injected doses. An average image related to the mean biodistribution of the radioimmunoconjugate in the total body was computed using the SIMIND Monte Carlo code [20]. This simulated image showed the relative uptake between tumour and the normal organs.

In general, activity (C) in the normal organs and regions of interest were computed according to the Siegel *et al.* suggestions [18], as:

$$C = \sqrt{\frac{I_a I_p}{\exp(-\mu d)}} \times \frac{1}{S}$$

where:

- I_a is the counts computed from the scatter-corrected anterior view
- I_p is the counts computed from the scatter-corrected posterior view
- $\exp(\mu d)$ represents the transmission factor across the region of interest and may be determined by measuring the ratio of the count rates I/I_o, obtained using a flood source with (I) and without (I_o) the patient in position
- S is the system calibration factor (count per unit activity), computed by counting a source of known activity in air.

Urinary excretion was evaluated by collecting samples of all the voided urine during the first 48 h post-injection. Volumes and times of all urinations were recorded and measured in duplicate using a ratemeter (SR8; Nuclear Enterprises, UK). The sample count rates were corrected for decay and expressed as a percentage of administered activity. Urinary excretion was reported as the total percent of injected doses.

Internal radiation dosimetry

The medical internal radiation dose formalisms at voxel and organ levels were used for internal radiation estimations in the tumour region and for the normal organs, respectively [21]. Three-dimensional dose distributions in the volume containing the surgically created resection cavity (SCRC) and brain adjacent tissue (BAT) were estimated using voxel-based methods. Time–activity curves and residence times were computed for each voxel, combining primary data of a single SPECT study and biological parameters obtained from multiple planar images [21]. The tomographic acquisition and processing protocols were addressed to quantitative single photon emission computed tomography analysis, according to suggestions by Hambye *et al.* [14].

The tomographic studies were acquired from all patients at 3 h post-injection, using 64 projections of 30 s each, a 64×64 matrix size and circular orbit. Collimator and energy windows settings were similar to the planar imaging conditions. Meanwhile, the acquisition protocols for planar studies followed the schedule described previously.

SPECT slices were reconstructed using the filtered back-projection method (Hamming–Hann filter). Scatter correction of the SPECT projections was performed using the triple-windows energy method and attenuation correction was also applied to all the studies using the Chang method [14].

Computations of three-dimensional dose distributions were performed using the TRIDOSE software package developed by our group using Interactive Data Language (IDL-Demo version 6.0). The input data were the quantitative SPECT slices, the S values at the voxel level for ^{188}Re, and complementary data related to biological and calibration parameters [22]. The calculation of the S values at the voxel level for ^{188}Re was performed using the methodology described by Cornejo *et al.* [23].

The three-dimensional dose distributions were estimated as:

$$D_{(\text{voxel } k)} = \sum_{h=0}^{N} \tilde{A}_{\text{voxel } h} \times S_{(\text{voxel } k \leftarrow \text{voxel } h)}$$

where:

- $D_{(\text{voxel } k)}$ is the total absorbed dose to the target voxel k from the N surrounding source voxels h
- $\tilde{A}_{\text{voxel } h}$ is the cumulated activity in the source voxel h
- $S_{(\text{voxel } k \leftarrow \text{voxel } h)}$ is the mean absorbed dose to a target voxel k per unit of cumulated activity in a source voxel h.

Mean and maximum values of the absorbed doses were calculated and reported in the tumour region by using volumes of interest (VOIs). The VOIs were created interactively over the dose distributions images, using isocontours or manual sequential regions of interest which included the SCRC volume and the BAT, defined as a slim area with a thickness ranged 1.5–2 cm bordering the SCRC. In order to estimate these VOIs, one set of magnetic resonance images was acquired from all patients one week before the immunoconjugate administration. Gadolinium-enhanced T1-weighted images were combined with T2-weighted images to define the volume of the SCRC plus the BAT by using the software package STASSIS developed at the International Centre of Neurological Restoration (CIREN), Havana, Cuba.

The MIRDOSE 3 software (free software from Oak Ridge Laboratories) was employed to compute the radiation doses received by the normal organs [24]. Source organ residence times were computed from their observed time–activity curves. Residence times in the urinary bladder were computed using a dynamic bladder model [12]. Mean absorbed doses were reported for the nine normal organs receiving the highest radiation doses and the total body.

Blood samples were collected at different times (0.5, 1, 2, 4, 6, 8, 12, 24 and 48 h post-injection) from all patients in order to estimate the absorbed dose to red marrow using the method of Sgouros *et al.* [25] and taking into account the suggestions of Cremonesi *et al.* [19]. The samples were placed in anti-coagulated tubes, measured in a ratemeter and expressed as a percentage of the administered activity. Regression analyses of the time–activity curves were performed and the residence times of ^{188}Re-nimotuzumab in red marrow were computed using a reduction factor of 0.3 to consider the difference in activity between blood and marrow [19].

Calibrations

Sets of calibration studies were carried out in order to complement the biodistribution and dosimetric calculations. The SPECT total performance, pixel size, sensitivity, attenuation coefficients and scatter correction were evaluated periodically before performing the scintigraphic studies.

Statistical analysis

Biodistribution and dosimetric results were reported as mean ± standard deviation (SD) for all the patients included. Regression analysis was carried out in order to fit the count–time curves to exponential functions of the source organs, using the Microcal Origin software package v6.0. Data were processed using several datasheets created with Microsoft Office Excel 2003 and SPSS for Windows (v12.0).

Results

Toxicity evaluations of the patients

Nine patients (two female and seven male, mean age 46.4 ± 16.0 years, mean weight 68.9 ± 15.1 kg and mean height 165.1 ± 5.6 cm) were included in this study. All had recurrent gliomas grade III or IV and fulfilled the inclusion criteria. Table 1 shows the features of all the patients included. Initially, three patients were enrolled in the 370 MBq dose level; no one presented significant adverse effects or signs of radiotoxicity. The only effects noted were light or moderated reactions such as headache, nausea, vomiting and light tremors which resolved in a short period. Significant alterations in the clinical laboratory parameters related to radiotoxicity of normal organs were not found or signs of haematological toxicity. Patient 3 showed a slightly increased glutamate–pyruvate transaminase index 14 days post-injection.

Table 1 Characteristics of the patients included in this study

Patient number	Sex	Age (years)	Weight (kg)	Height (cm)	Dose level	Tumour grade	Localization
1	M	53	55	160	I	GM	Tem-Occ-R
2	M	20	54	165	I	GM	Par-Occ-R
3	F	25	54	164	I	AA	Fro-Par-L
4	F	65	61	162	II	GM	Fro-Par L
5	M	62	96	172	II	GM	Par-Occ-R
6	M	54	75	170	II	GM	Par-Occ-L
7	M	53	63	159	I	GM	Par-Occ-R
8	M	35	77	160	I	GM	Fro-R
9	M	51	85	174	I	GM	Tem-Occ-L

GM, Glioblastoma multiforme; AA, anaplastic astrocitoma; Tem, temporal; Occ, occipital; Fro, frontal; Par, parietal; R, right; L, left.

The dosimetric calculations demonstrated that it was not due to the ^{188}Re-nimotuzumab liver uptake.

Later, three patients were included in the 555 MBq dose level; the first patient presented moderated adverse effects similar to the previously described but the second had severe adverse reactions consisting of generalized convulsions and vomiting, which required medication, for 3 days. A third patient was then enrolled who also presented severe adverse effects including a worsening of his pre-existing motor defects. No haematological toxicity or signs of radiotoxicity were found in other normal organs of these two patients.

Taking into account that two-thirds of the patients included in the 555 MBq dose level presented severe adverse effects, three patients were additionally included in the previous dose level. No significant signs of radiotoxicity were observed. Patients 8 and 9 showed light adverse effects, consisting of headache and nausea, which were resolved quickly and without medication. No immune response (HAMA titres) against the humanized monoclonal antibody nimotuzumab was detected in any patient included. According to the described results the maximum tolerated dose of this study was 370 MBq of ^{188}Re-nimotuzumab.

Biodistribution

The biodistribution studies included the processing and evaluation of at least 98 static images per patient, including the emission, scatter and transmission acquired data. Figure 1 illustrates a set of planar views of the distribution of ^{188}Re-nimotuzumab in the total body of patient no. 4 at 1, 5, 24 and 48 h post-injection. These geometric mean images were previously processed including attenuation and scattering corrections.

A set of whole-body images containing the mean biodistribution of this compound were computed using the real biological data estimated from the planar views and taking into account the measurement conditions during the studies (Fig. 2). These simulated images, obtained with the SIMIND Monte Carlo code, show the relative uptake of ^{188}Re-nimotuzumab among the tumour region and the main source organs.

Fig. 1

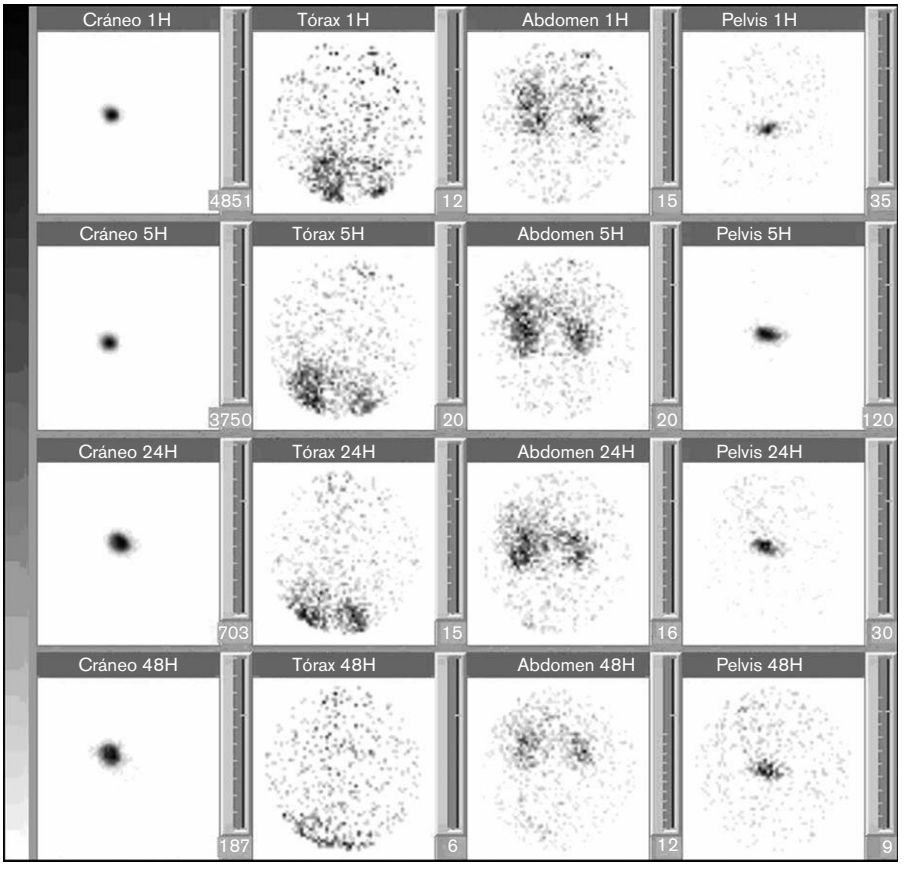

Processed static views (geometric mean) of head, chest, abdomen and pelvis acquired from patient 4 at 1, 5, 24 and 48 h.

Fig. 2

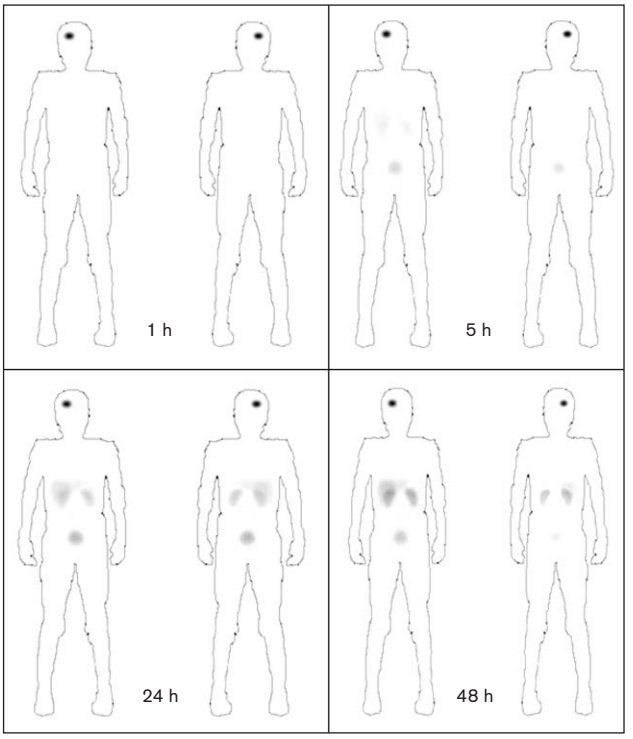

Mean biodistribution of 188Re-nimotuzumab in total body at 1, 5, 24 and 48 h. These images were simulated providing the measured biological data and γ camera parameters to the SIMIND software.

Fig. 3

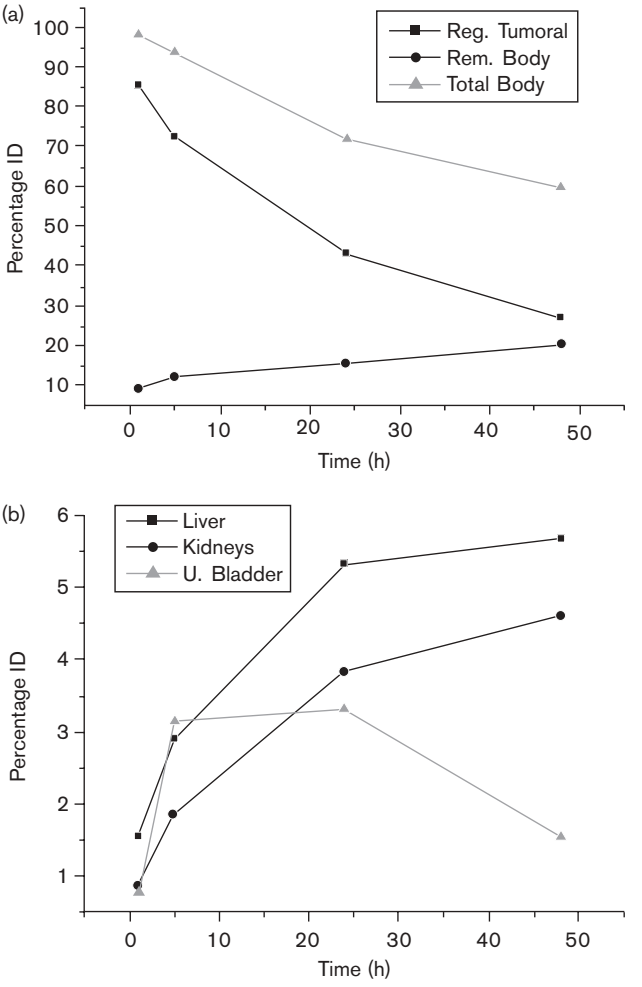

Mean biological clearance curves for (A) tumoural region (Reg. Tumoural); remainder of body (Rem. Body) and total body; and (B) liver, kidneys and urinary bladder (U. Bladder). Data are corrected for decay.

The visual inspection of the processed scintigraphic images and the biodistribution calculations revealed that ^{188}Re-nimotuzumab was retained in the tumour cavity and adjacent malignant tissues for a long period. One hour after the injection it was calculated that approximately 85.5 ± 10.3% of nimotuzumab was in the tumour cavity and adjacent tissues with a biological half-life of approximately 22.7 ± 8.9 h.

The activity cleared from the SCRC was distributed among the normal organs, according to the expected patterns: liver, kidneys and urinary bladder showed a minimal activity uptake on almost all patients. The mean biological clearance curves for these organs are shown in Fig. 3. Liver and kidneys presented an increased uptake versus time, reaching maximum values of 5.6 and 4.6%ID, respectively, at 48 h post-injection. The urinary bladder presented a non-negligible uptake showing that urine was the main clearance pathway of this compound. The maximum accumulation of ^{188}Re-nimotuzumab in urinary bladder was around 3.3%ID, assessed from the 24 h set images. On the other hand, it was estimated from the analysis of urine time–activity curves that approximately 6.2 ± 0.8%ID was excreted during the first 48 h post-administration.

Two patients showed specific biodistribution patterns with high uptakes of the radioimmunoconjugate being found in the spinal cord of patients 6 and 7, reaching maximum values of 4.2 and 5.3%ID, respectively, at 5 h post-injection. These uptake values were related to an unexpected ^{188}Re-nimotuzumab leakage into the brain ventricles of both patients.

Tumour dosimetry

Three-dimensional dose distributions in the tumour region were computed for all patients. The mean and maximum absorbed doses computed from the selected VOIs are reported in Table 2. Some other parameters of interest such as the VOIs volume, the estimated percent of injected dose on the tumour region at 1 h post-injection (without decay correction) and its effective half-life are also reported.

Table 2 The mean and maximum absorbed doses in the tumour region computed from the selected volumes of interest

Patient number	Group	Volume of interest (cm^3)	%ID 1 h post-injection[a]	Effective half-life (h)	Mean dose (Gy)	Maximun dose (Gy)
1	I	96.5	89.0	7.5	19.9	42.8
2	I	56.9	90.3	8.7	24.8	53.2
3	I	78.3	63.6	11.4	25.6	57.5
4	II	84.9	83.2	11.3	36.5	79.3
5	II	85.5	76.7	9.8	32.7	75.1
6	II	69.8	70.3	7.2	24.0	52.6
7	I	73.3	91.3	10.9	28.1	58.9
8	I	110.4	90.4	9.7	21.5	46.1
9	I	78.3	83.8	7.6	24.4	52.2

[a]Data are not corrected for decay.

Fig. 4

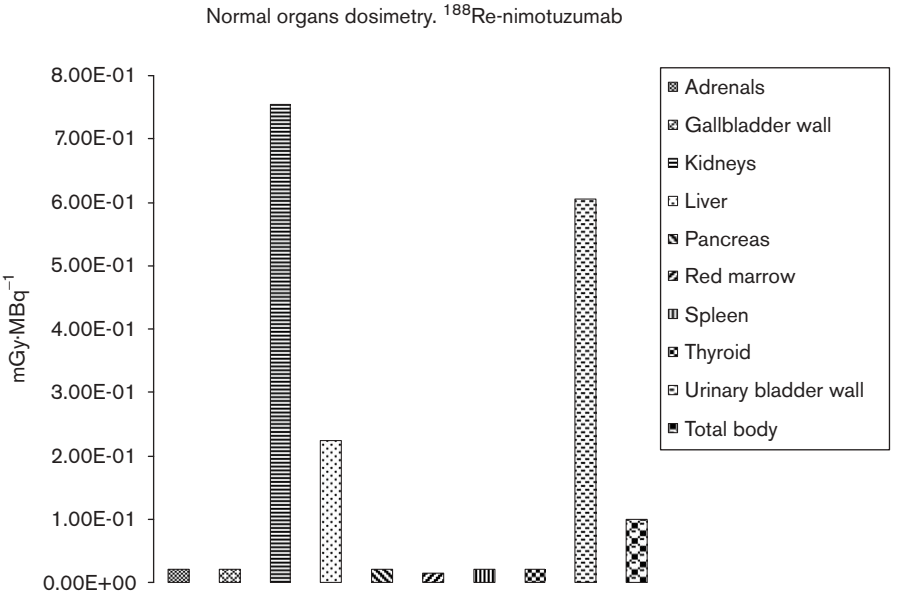

Mean absorbed doses received by the most irradiated normal organs.

The average of the mean absorbed doses in groups I and II were 24.1 ± 2.9 and 31.1 ± 6.4 Gy, respectively, while the maximum doses received in the tumour region were 58.9 Gy in group I and 79.3 Gy in group II. The computed absorbed doses showed variability among the patients of the same dose level; these differences were higher in group II.

The volume of the VOIs, which included the SCRC plus the BAT, ranged from 56.9 to 110.4 cm^3 and the effective half-life of the ^{188}Re-nimotuzumab in this region was around 9.4 ± 1.6 h. The radioimmunoconjugate uptake in the tumour region also showed a wide variety of values ranging from 63.6 to 91.3%ID at 1 h post-injection and they decreased showing different half-life during the next 48 h.

Dosimetry of normal organs

The absorbed doses received by 25 target organs were computed and averaged for all patients. Residence times were calculated from the time–activity curves of brain, liver, kidneys, urinary bladder and remainder of body, and used as input data to MIRDOSE software. It was assumed that the activity in the SCRC and BAT was distributed homogeneously in the total brain in order to estimate its contribution to the irradiation of the normal organs. Sawtooth-shaped excretion curves were obtained from seven patients when the dynamic bladder model was applied to estimate the urinary bladder residence times.

The mean absorbed doses received by total body and the eight most irradiated organs are illustrated in Fig. 4. All these organs (adrenals, gallbladder wall, kidneys, liver, pancreas, red marrow, spleen, thyroid and urinary bladder) received more than 0.15 $mGy \cdot MBq^{-1}$. As expected, the higher absorbed doses were estimated to the sources organs; kidneys, liver and urinary bladder received 0.754, 0.223 and 0.604 $mGy \cdot MBq^{-1}$, respectively. The mean absorbed dose received by the total

Fig. 5

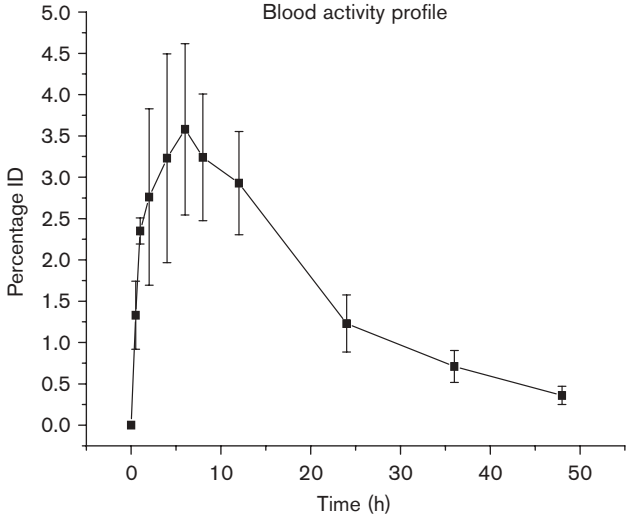

Mean curve of blood activity at different time intervals.

body was around 0.0996 mGy·MBq^{-1} while the estimated equivalent and effective doses were 0.323 and 0.126 mSv·Bq^{-1}, respectively.

The calculations of the absorbed doses in red marrow were also estimated based on the analysis of activity in blood. The mean curve computed from the activity in blood versus time showed an exponential uptake phase reaching the maximum value at 6 h post-injection and a fast exponential decay with a half-life of 13.1 h (Fig. 5). The residence time of the ^{188}Re-nimotuzumab in red marrow was estimated around 0.05 h producing a self dose in the order of 0.0093 mGy·MBq^{-1}. Therefore, patients included in the first and second groups received absorbed doses around 3 and 5 mGy, respectively, on this critical organ. It could be noted that the contribution of the activity in blood to the absorbed doses in red marrow was slightly lower than the contribution of the activity in the remainder of body which was estimated about 6 and 9 mGy, in that order, for groups I and II.

Calibration studies

The calibration studies provided complementary information for the processing of the biodistribution and dosimetric studies. First, the whole set of quality control tests for planar and SPECT studies were performed to ensure the correct functioning of the system. All tests were carried out according to the institutional quality control program. The voxel size evaluation showed a mean value of 6.8 mm (matrix format of 64×64), the SPECT sensibility and the attenuation correction coefficients were estimated for ^{188}Re previous to starting patient inclusion using a Carlsson phantom. The triple-windows energy technique was implemented and optimized for the scattering correction of the planar and SPECT studies using an Alderson anthropomorphic phantom.

Discussion and conclusion

In the present study, the new radioimmunoconjugated ^{188}Re-nimotuzumab has been evaluated for the loco-regional radioimmunotherapy of high-grade gliomas. A phase I clinical trial was performed to evaluate the toxicity, biodistribution and dosimetry of this compound. The well-know overexpression of EGFr in gliomas [26], the documented high affinity of nimotuzumab for this antigen and its reported low immunogenicity [9–11] suggested a potential use of this humanized MAb labelled with ^{188}Re for radionuclide therapy of these aggressive tumours. The radionuclide ^{188}Re was selected due to its ideal physical features for radionuclide therapy, the generator availability and easy labelling procedures [14]. The labelling methodology for ^{188}Re-nimotuzumab is well established and optimized [16], taking into account previous experiences [27], and pre-clinical evaluations demonstrated the potential efficacy and safety of this radioimmunoconjugate [13]. Prior preclinical studies showed that in-vitro and in-vivo stability of the ^{188}Re-labelled nimotuzumab was similar to ^{99m}Tc-nimotuzumab [16]. Challenge against a 300-fold molar excess of L-cysteine showed analogous stability of both compounds. Perera *et al.* [16] also evaluated the biodistribution of ^{188}Re-nimotuzumab in 20 male Wistar rats demonstrating a similar in-vivo stability of ^{188}Re-nimotuzumab and ^{99m}Tc-nimotuzumab.

The present study found that the maximum tolerated dose of ^{188}Re-nimotuzumab was about 370 MBq. Three patients were initially included at this dose level with no evidence of severe adverse effects, and similar results were obtained in the last three patients who received the same radioimmunoconjugate activity. However, two of the three patients at the 555 MBq level presented severe adverse events, not allowing escalation to the next dose level. In spite of the fact that the mean absorbed doses estimated in the tumour regions were higher for patients included in the second dose level (24.1 ± 2.9 Gy vs. 31.1 ± 6.4 Gy), the adverse events in these patients may not be completely related to radiotoxicity induced by irradiation of cerebral tissue. They may also be related to the brain oedema produced by an increment in the intracranial pressure which was detected in both patients. Coincidentally, in these two patients, there was unexpected intraventricular access of this radioimmunoconjugate from the surgically created resection cavity, allowing ^{188}Re-nimotuzumab to pass into the cerebrospinal fluid. In a previous study the intratumoural infusion of a murine anti-EGFr MAb (MAb 425) in patients with advanced malignant glioma produced severe

inflammatory reactions, limiting the treatment of patients with the total intended dose [28]. On the other hand, several clinical trials have reported mean absorbed doses in the walls of the surgically created resection cavity in the range of 150–300 Gy [2]. Thus, the doses received by the patients in our clinical trial could not have induced the detected adverse events. However, no patients were allowed to receive higher dose activities, according to the dose escalation scheme.

Dosimetric calculations showed variability of the absorbed doses in the tumour region among the patients, particularly significant in the second dose level. These results are closely related to the dependence of the absorbed doses with the resection cavity volume; the percent of injected dose accumulated in the tumour region and the effective half-life or activity cleared from it. These factors led to mean tumour absorbed doses between 24.0 and 36.5 Gy in the patients at the 555 MBq dose level. Similar variability was found and described by Akabani *et al.* [29].

As expected, the normal organs receiving the higher percentages of activity cleared from tumour were kidneys, urinary bladder and liver. Previous studies demonstrated similar biodistribution for ^{99m}Tc-nimotuzumab due the well-known EGFr overexpression in liver (about 10^4 molecules per cell) and high nimotuzumab urinary excretion [12]. No abnormal biodistribution pattern was found in any patient, corresponding either to free perrhenate (thyroid or stomach activity) or radiocolloids (spleen activity), thus demonstrating the in-vivo stability of the radiopharmaceutical.

Kidneys, urinary bladder and liver also received the higher total absorbed doses, but the computed values (around 420, 330 and 130 mGy, respectively) were lower than the reported limits that induce radiotoxicity. On the other hand, the red marrow irradiation from normal organs and blood produced low absorbed doses. Less than 10 mGy of absorbed dose was estimated in red marrow, which is due to the small amount of activity cleared from the tumour region.

The results of this study showed the safety of loco-regional administration of ^{188}Re-nimotuzumab to patients bearing high-grade gliomas and its potential effectiveness for the treatment of this malignant disease. High absorbed doses can be delivered to the tumour region using these procedures without a significant irradiation of normal organs. It could produce tumouricidal doses in the BAT area avoiding the probability of recurrence in patients with these neoplasms. The effective half-life of ^{188}Re-nimotuzumab in the tumour region, the mean and maximum absorbed doses, for example, suggest the use of a fractionated treatment similar to the schemes proposed by several groups [3,30]. The patients to be included in these studies should be carefully selected in order to avoid unsuspected extra-tumour activity and its undesirable consequences. Finally, we consider that the efficacy of this radioimmunoconjugate should be evaluated in a phase II clinical trial.

Acknowledgements

The authors would like to thank Zaida Amador, Rafael Rodriguez, Miguel Puig, Jose A. Rodriguez, Barbara Estupiñan, Marilyn Pérez, Addys Gonzalez, Nestor Cornejo and Normando Iznaga for their contribution in the data acquisition, patient management and complementary tasks during the clinical studies and the preparation of the paper. We would also like thank Professor Frederic Fahey from the Children's Hospital, Boston, USA, for his kind support in editing our paper.

References

1 Paganelli G, Bartolomei M, Grana C, Ferrari M, Rocca P, Chinol M. Radioimmunotherapy of brain tumour. *Neurol Res* 2006; **28**:518–522.
2 Zalutsky MR. Current Status of therapy of solid tumours: brain tumour therapy. *J Nucl Med* 2005; **46**:151S–156S.
3 Riva P, Franceschi G, Riva N, Casi M, Santimaria M, Adamo M. Role of nuclear medicine in the treatment of malignant gliomas: the locoregional radioimmunotherapy approach. *Eur J Nucl Med* 2000; **27**:601–609.
4 Reardon DA, Akabani G, Coleman RE, Friedman AH, Friedman HS, Herndon JE II, *et al.* Salvage radioimmunotherapy with murine iodine-131-labelled antitenascin monoclonal antibody 81C6 for patients with recurrent primary and metastatic malignant brain tumours: phase II study results. *J Clin Oncol* 2006; **24**:115–122.
5 Mamelak AN, Rosenfeld S, Bucholz R, Raubitschek A, Nabors LB, Fiveash JB, *et al.* Phase I single-dose study of intracavitary-administered ^{131}I-TM-601 in adults with recurrent high-grade glioma. *J Clin Oncol* 2006; **24**:3644–3650.
6 Epenetos AA, Courtenay-Luck N, Pickering D, Hooker G, Durbin H, Lavender JP, *et al.* Antibody guided irradiation of brain glioma by arterial infusion of radioactive monoclonal antibody against epidermal growth factor receptor and blood group A antigen. *BMJ* 1985; **290**:1463–1466.
7 Quang TS, Brady LW. Radioimmunotherapy as a novel treatment regimen: ^{125}I-labelled monoclonal antibody 425 in the treatment of high-grade brain gliomas. *Int J Rad Oncol Biol Phys* 2004; **58**:972–975.
8 Mateo C, Moreno E, Amour K, Lombardero J, Harris W, Perez R. Humanization of a mouse monoclonal antibody that blocks the epidermal growth factor receptor: recovery of antagonistic activity. *Immunotechnology* 1997; **3**:71–81.
9 Torres LA, Perera A, Batista JF, Hernandez A, Crombet T, Ramos M, *et al.* Phase I/II clinical trial of the humanized anti-EGF-r monoclonal antibody h-R3 labelled with ^{99m}Tc in patients with tumour of epithelial origin. *Nucl Med Commun* 2005; **26**:1049–1057.
10 Crombet T, Torres L, Neninger E, Catala M, Perera A, Torres O, *et al.* Pharmacological evaluation of the humanized anti-epidermal growth factor receptor monoclonal antibody, h-R3, in patients with advance epithelial cancer. *J Immunother* 2003; **26**:139–148.
11 Crombet T, Ramos M, Osorio M, Cruz T, Roca C, del Castillo R, *et al.* Use of the humanized anti-epidermal growth factor receptor monoclonal antibody h-R3 in combination with radiotherapy in the treatment of locally advanced head and neck cancer patients. *J Clin Oncol* 2004; **22**:1646–1654.
12 Iznaga-Escobar N, Torres L, Morales A, Ramos M, Rodríguez N, Pérez N, *et al.* ^{99m}Tc-labelled anti-human Epidermal Growth Factor Receptor Antibody (ior egf/r3) in patients with tumour of epithelial origin: II. Pharmacokinetics and clearances. *J Nucl Med* 1998; **39**:1918–1927.
13 Gonzalez B, Casaco A, Alvarez P, Leon A, Santana E, Bada A, *et al.* Local and systemic toxicity of h-R3, an anti-epidermal growth factor receptor monoclonal antibody, labelled with ^{188}osmiun after the intracerebral administration in rats. *Exp Toxicol Pathol* 2005; **56**:313–319.
14 Hambye ASE, Dobbelier AA, Vervaet AM, Knapp FF. Image quality with ^{188}Re and ^{99m}Tc: Comparative planar and SPECT evaluation in a phantom study and implications for dosimetry. *World J Nucl Med* 2002; **1**:12–20.

15 Lamberta B, Klerkb JMH. Clinical applications of ^{188}Re-labelled radiopharmaceuticals for radionuclide therapy. *Nucl Med Commun* 2006; **27**:223–229.
16 Perera A, Leyva R, Gamboa R, Alberdi L, Xiques A. Marcaje del anticuerpo monoclonal humanizado h-R3 con ^{188}Re. *Nucleus* 2003; **33**:64–68.
17 Schwarz A, Steinstraber A. A novel approach to ^{99m}Tc-labelled monoclonal antibodies. *J Nucl Med* 1987; **28**:721.
18 Siegel JA, Thomas SR, Stubbs JB, Stabin MG, Hays MT, Koral KF *et al*. MIRD pamphlet no. 16: techniques for quantitative radiopharmaceutical biodistribution data acquisition and analysis for use in human radiation dose estimates. *J Nucl Med* 1999; **40**:37S–61S.
19 Cremonesi M, Ferrari M, Chinol M, Stabin MG, Grana C, Prisco G, *et al*. Three-step radioimmunotherapy with ^{90}Y-biotin: dosimetry and pharmacokinetics in cancer patients. *Eur J Nucl Med* 1999; **26**:110–120.
20 Ljungberg M, Larsson A, Johansson L. A New collimator simulation in SIMIND based on the delta-scattering technique. *IEEE Trans Nucl Sci* 2005; **52**:1370–1375.
21 Bolch WE, Bouchet LG, Robertson JS, Wessels BW, Siegel JA, Howell RW, *et al*. The dosimetry of nonuniform activity distributions – radionuclide S values at the voxel level. MIRD Pamphlet No. 17. *J Nucl Med* 1999; **40**:11–36.
22 Torres LA, Coca MA, Cornejo N. A Software package for tridimentional patient-specific dosimetry in ^{188}Re labelled h-R3 locoregional RIT. In: *Proceedings of IAEA International Conference on Quality Assurance and New Techniques in Radiation Medicine. IAEA-CN-146*. Vienna: IAEA; 2006. pp. 92–94.
23 Cornejo N, Coca MA, Torres LA. Cálculo de valores 'S' para ^{188}Re en una geometría voxel. *Revista de Física Médica* 2006; **7**:101–106.
24 Stabin MG. MIRDOSE – the personal computer software for internal dose assessment in nuclear medicine. *J Nucl Med* 1996; **37**:538–546.
25 G; Stabin M, Erdi Y, Akabani G, Kwok C, Bertrand BA, *et al*. Red marrow dosimetry for radiolabelled antibodies that bind to marrow, bone, or blood components. *Med Phys* 2000; **27**:2150–2164.
26 Eller JL, Longo SL, Hicklin DJ, Canute GW. Activity of anti-epidermal growth factor receptor monoclonal antibody c225 against glioblastoma multiforme. *Neurosurgery* 2002; **51**:1005–1014.
27 Iznaga-Escobar N. Direct radiolabeling of monoclonal antibodies with rhenium-188 for radioimmunotherapy of solid tumors – a review of radiolabeling characteristics, quality control and in vitro stability studies. *Appl Radiat Isot* 2001; **54**:399–406.
28 Wersall P, Ohlsson I, Biberfeld P, Collins VP, Krusenstjerna S, Larsson S, *et al*. Intratumoural infusion of the monoclonal antibody, mAb 425, against the epidermal-growth-factor receptor in patients with advanced malignant glioma. *Cancer Immunol Immunother* 1997; **44**:157–164.
29 Akabani G, Cokgor I, Coleman RE, Gonzalez D, Wong TZ, Friedman AS, *et al*. Dosimetry and dose-response relationships in newly diagnosed patients treated with ^{131}I-labelled anti-tenascin monoclonal antibody 81C6 therapy. *Int J Rad Oncol Biol Phys* 2000; **46**:947–958.
30 Goetz C, Riva P, Poepperl G, Gildehaus FJ, Hischa A, Tatsch K, *et al*. Locoregional radioimmunotherapy in selected patients with malignant glioma: experiences, side effects and survival times. *J Neurooncol* 2003; **62**:321–328.